Available online at www.sciencedirect.com
SCIENCE DIRECT®
Journal of Solid State Chemistry 170 (2003) 24–29
JOURNAL OF SOLID STATE CHEMISTRY
http://elsevier.com/locate/jssc

High-pressure synthesis, crystal structure and magnetic properties of a new cuprate $(Nd,Ce)_{2+x}CaCu_2O_{6+y}$

N.D. Zhigadlo,[1] K. Kimoto, M. Isobe, Y. Matsui, and E. Takayama-Muromachi*

National Institute for Materials Science (NIMS), 1-1 Namiki, Tsukuba, Ibraki 305-0044, Japan

Received 8 February 2002; received in revised form 3 June 2002; accepted 5 August 2002

Abstract

New phase $(Nd,Ce)_{2+x}CaCu_2O_{6+y}$ was prepared at a high-pressure/high-temperature condition of 6 GPa and 1300°C. It had a nonstoichiometric composition close to $Nd_{2.16}Ce_{0.225}CaCu_2O_{6+y}$. According to X-ray diffraction pattern, the $Nd_{2.16}Ce_{0.225}CaCu_2O_{6+y}$ phase has a tetragonal lattice with $a = 3.845(1)$ Å, $c = 19.349(5)$ Å. However, electron microscopic observations revealed a complicated shear structure for this phase. Magnetic susceptibility and magnetic hysteresis measurements were performed for the $Nd_{2.16}Ce_{0.225}CaCu_2O_{6+y}$ sample and it was found that the phase undergoes a weak ferromagnetic transition at 150 K. Below $\approx$40 K, complicated magnetic behavior was observed suggesting the presence of second weak ferromagnetic transition near 40 K.

Keywords: High-pressure synthesis; (Nd; $Ce)_{2+x}CaCu_2O_{6+y}$; HRTEM; Weak ferromagnetic transition

1. Introduction

Since the discovery of high-temperature superconductivity in the La–Ba–Cu–O system [1], a large number of cuprate superconductors have been found. Their common structural characteristic is the presence of the CuO_2 plane. The 0212-type phases of $R_2ACu_2O_6$ (R: rare earth, A: alkaline earth) [2–4] attracted much attention, because they have a simple structure with double CuO_2 layers similar to the $RBa_2Cu_3O_7$ superconductors. Although the 0212-type phases prepared under ambient pressure is not superconducting, high oxygen pressure treatment is effective to induce superconductivity in $(La,Sr)_2CaCu_2O_6$ [5], $(La,Ca)_2CaCu_2O_6$ [6], etc.

High-pressure synthesis technique has been recognized to be a powerful method in the search for new high-T_c oxide superconductors. Recently, Isobe et al. [7] found a new 0212-type cuprate $Nd_2CaCu_2O_6$ under high pressure. Its structure is schematically shown in Fig. 1. Carrier doping was tried for this phase by partial substitution of Sr for Nd and weak superconducting signal was observed at 18 K in the $Nd_{1.6}Sr_{0.4}CaCu_2O_6$ sample [7].

In the present study, we performed phase search experiments for the Ce-containing system of Nd–Ce–Ca–Cu–O using high-pressure synthesis technique. The Ce-doping brought about unexpected effects and a new phase of $(Nd,Ce)_{2+x}CaCu_2O_{6+y}$ was formed. X-ray diffraction pattern suggested that it was isostructural to $Nd_2CaCu_2O_6$. However, electron microscopic observations revealed that it has a complicated shear structure. Moreover, it showed weak ferromagnetic transition. High-pressure synthesis, and the structural and magnetic properties of the new Ce-containing phase are presented.

2. Experimental

Nd_2O_3 (99.9%), CeO_2 (99.9%), Ca_2CuO_3 and CuO (99.9%) were used to obtain nominal mixtures for high-pressure synthesis. Nd_2O_3 and CeO_2 powders were heated at 1000°C for 24 h before using. Single-phase Ca_2CuO_3 was synthesized through solid state reaction of CuO and $CaCO_3$ at 1000°C for 5 days with several

*Corresponding author. Fax: +81-298-58-5650.
E-mail address: muromachi.eiji@nims.go.jp (E. Takayama-Muromachi).
[1] Present address: Institute of Solid State and Semiconducting Physics, P. Brovki 17, Minsk 220072, Belarus.

0022-4596/03/$ - see front matter © 2002 Elsevier Science (USA). All rights reserved.
PII: S0022-4596(02)00011-7

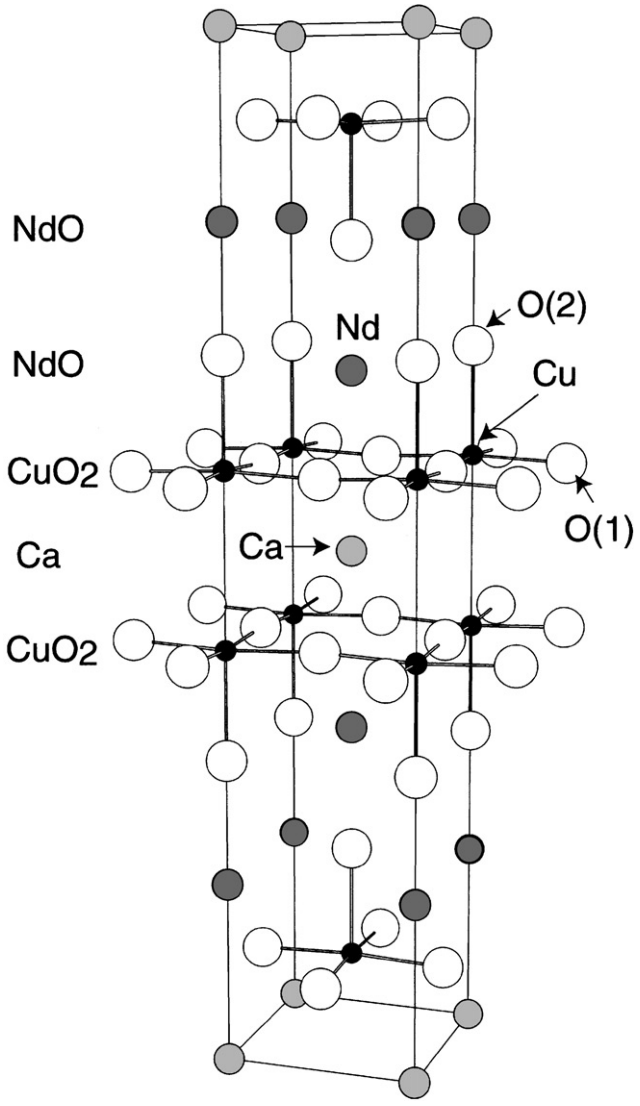

Fig. 1. Crystal structure of $Nd_2CaCu_2O_6$.

intermediate grindings. The mixture was sealed in a gold capsule after being pulverized well, then was allowed to react in a belt-type high-pressure apparatus at 6 GPa and 1300°C. After heat treatment for 1–3 h, the sample was quenched to room temperature before the pressure was released. To check possible oxygen loss, the gold capsule was weighed before and after the high-pressure treatment.

The X-ray powder diffraction data were collected by a diffractometer (Philips, PW 1800) with CuK_α radiation over the range $2\theta = 2$–$70°$. The lattice parameters were determined by the least-squares refinements. Electron diffraction patterns and lattice images were taken using a high-resolution transmission electron microscope (HRTEM, Hitachi H-1500) operated at 800 kV. Electron-probe microanalysis (EPMA) was carried out using an analyzer (JEOL JXA-8600MX). In EPMA, a small ceramic specimen was well polished to obtain a surface with $\approx 2 \times 2\,mm^2$, and five to ten relatively large grains were selected and analyzed. Magnetic properties were measured using a commercial DC SQUID magnetometer (Quantum Design, MPMS).

3. Results and discussion

More than 30 starting mixtures having different cation compositions in the Nd–Ce–Ca–Cu–O system were tested at the high-pressure/high-temperature condition. In particular, a cross section of Ca:Cu = 1:2 in the pseudoquarternary diagram was studied most intensively. In the Nd–Ce–Ca–Cu–O system, there exist at least four phases which contain both Nd and Cu. The first one is Nd_2CuO_4 (or $(Nd,Ce)_2CuO_4$) with a T′-type structure [8]. The second phase $NdCuO_{2.5}$ [9] is

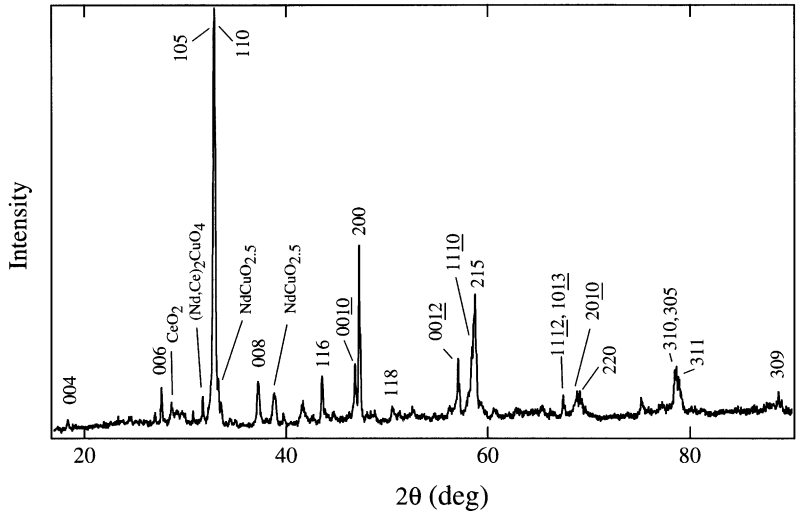

Fig. 2. X-ray powder diffraction pattern of the $Nd_{2.16}Ce_{0.225}CaCu_2O_{6.69}$ sample. Indices are given on the basis of a tetragonal lattice with lattice parameters of $a = 3.845(1)$ Å, $c = 19.349(5)$ Å.

essentially isostructural to an ordered oxygen-deficient perovskite $LaCuO_{2.5}$ [10, 11], but has a more distorted structure with a different symmetry due to the smaller size of the Nd ion. The third phase is $Nd_2CaCu_2O_6$ [7] described previously. The fourth phase is a new one and the best phase purity was attained from the nominal composition of $Nd_{2.16}Ce_{0.225}CaCu_2O_{6.69}$. Hereafter, we call this phase as 0212-(Nd,Ce).

Fig. 2 shows powder X-ray pattern of the $Nd_{2.16}Ce_{0.225}CaCu_2O_{6.69}$ sample. The main peaks of the pattern can be indexed on the basis of a tetragonal lattice with $a = 3.845(1)$ Å and $c = 19.349(5)$ Å. These dimensions suggest that the 0212-(Nd,Ce) phase has a $R_2CaCu_2O_6$-related structure. Major impurities included in this sample were Nd_2CuO_4, $NdCuO_{2.5}$ and CeO_2. To determine cation composition of this new phase, the $Nd_{2.16}Ce_{0.225}CaCu_2O_{6.69}$ sample was analyzed by EPMA. The composition obtained is $Nd_{2.37}Ce_{0.26}Ca_{0.96}Cu_2O_{6+y}$ which is close to the nominal value, though the Nd content is slightly higher compared with the nominal value. According to this result we adjusted the starting composition to the EPMA data, but the phase purity was not improved and the sample in Fig. 2 is, at the present stage, our best one for the 0212-(Nd,Ce) phase.

The $Nd_{2.16}Ce_{0.225}CaCu_2O_{6.69}$ sample was observed by HRTEM. Fig. 3 shows electron diffraction patterns of the 0212-(Nd,Ce) phase for (*hk*0), (*h*-*hl*) and (*hhl*) sections. The main strong spots in these patterns are consistent with the tetragonal lattice observed by the X-ray diffraction. In the (*h*-*hl*) diffraction pattern, only spots with $l = 10n$ are observed clearly. The 0010 index corresponds to the average plane–plane distance in the $Nd_2CaCu_2O_6$ structure (note that this structure contains 10 metal planes per *c*-length). On the other hand, $l = 2n$ spots are observed in the (*hhl*) section.

The striking feature of the electron diffraction patterns is the existence of many additional spots along the [110] direction. In Fig. 4, HRTEM image projected along [1,−1,0] is presented. A column-like pattern is seen in the image and each column includes rows consisting of five metal atoms. According to the lattice image, a structure model was constructed as shown in Fig. 5. This model presents a shear structure derived from the 0212-type structure shown in Fig. 1 with shear planes running parallel to the (1 1 0) plane. The interval

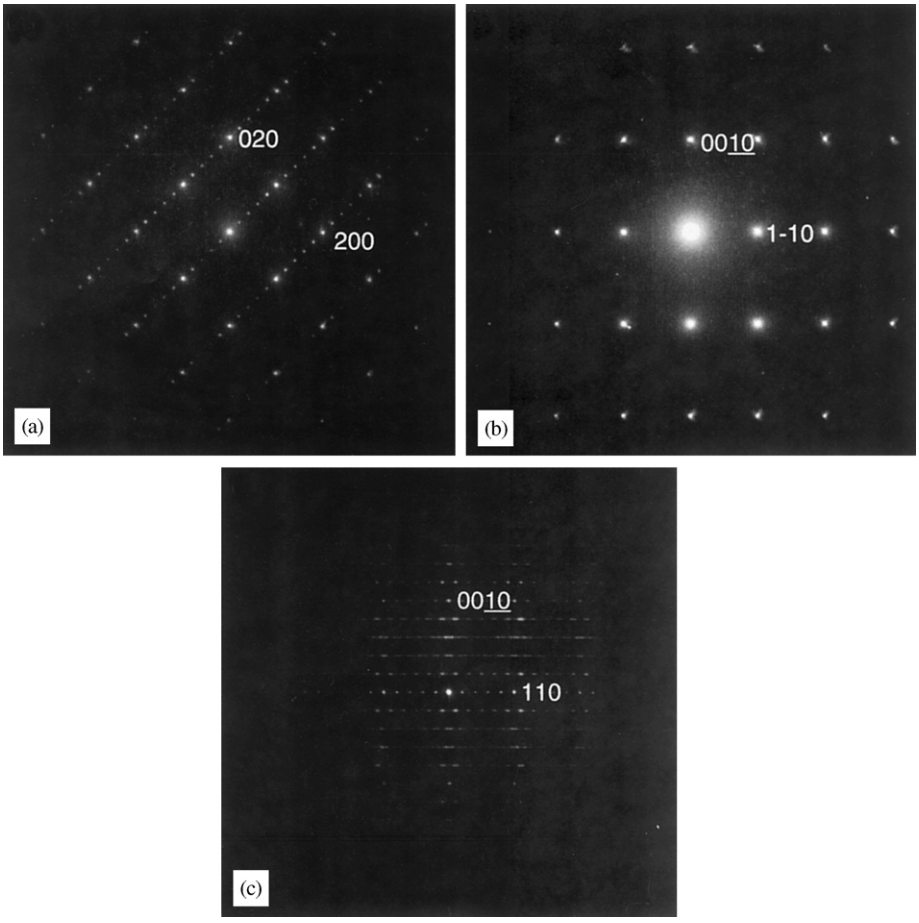

Fig. 3. The (a) (*hk*0), (b) (*h*−*hl*) and (c) (*hhl*) sections of the electron diffraction patterns of the 0212-(Nd,Ce) phase. Indexes given are based on the simple tetragonal cell.

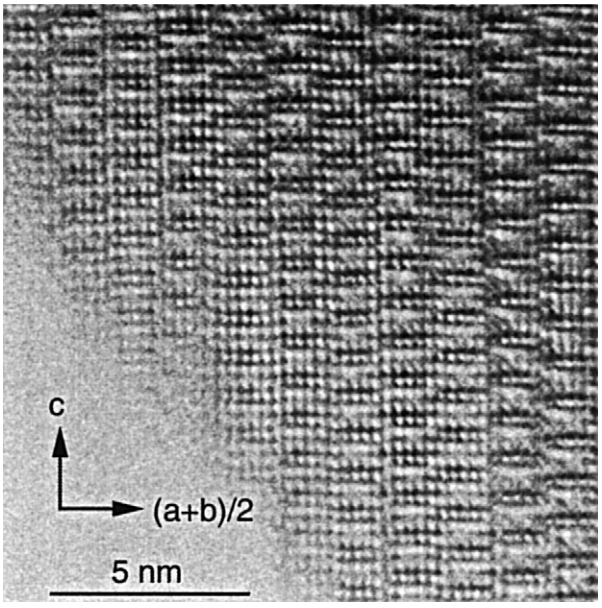

Fig. 4. HRTEM image projected along the [1–10] direction for the 0212-(Nd,Ce) phase.

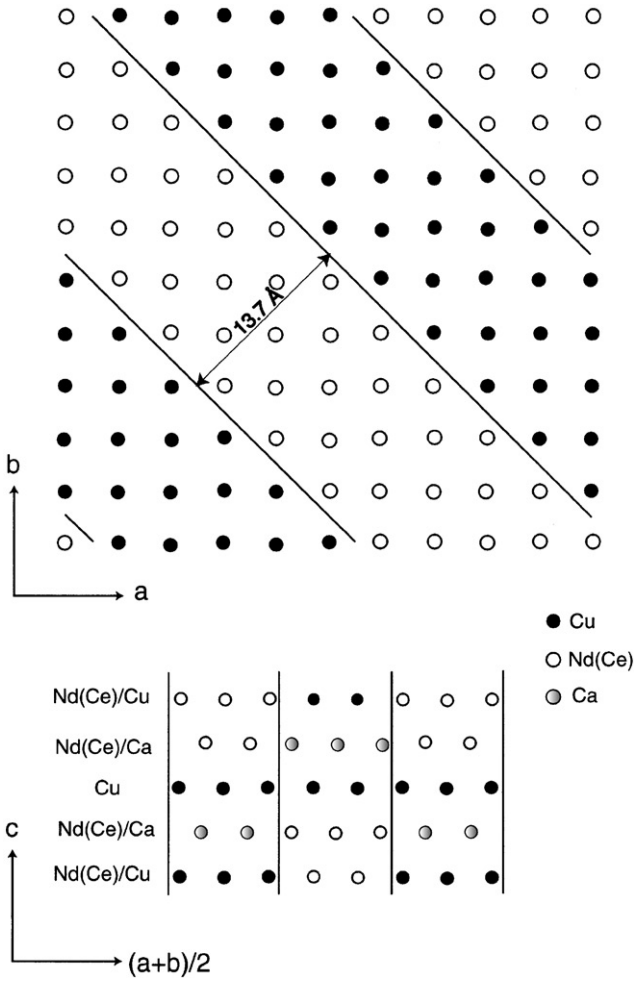

Fig. 5. Shear structure model for 0212-(Nd,Ce) phase.

of the shear plane is 13.7 Å forming the column with a width of 13.7 Å.With reference to an arbitrary column, atom positions in its adjacent column shift by $\approx c/5$. The atoms of the next column revert to the reference positions, resulting in a periodicity of 2×13.7 Å. By such a shear, the Nd(Ce) plane is interposed by the Cu or Ca planes (see the upper part of Fig. 5). It is, however, worth noting that in spite of the shear, the CuO_2 plane exists without the interposition as shown in the lower part of Fig. 5.

According to the shear structure model, the composition of the 0212-(Nd,Ce) phase becomes $(Nd,Ce)_2CaCu_2O_{6+y}$. However, the synthesis experiments and the EPMA measurements indicated that the real composition is $(Nd,Ce)_{2+x}CaCu_2O_{6+y}$ with $x \approx 0.4$. This result suggests that the structure near the shear plane is more or less irregular with the mutual mixing of (Nd,Ce), Ca and Cu atoms.

The structure model in Fig. 5 gives superlattice of $a_s = 5.4$ Å $b_s = 27.4$ Å and $c_s = 19.3$ Å, and this lattice is related to the fundamental tetragonal one as $a_s = \sqrt{2}a$, $b_s = 5\sqrt{2}b$, $c_s = c$. However, the diffraction pattern in Fig. 3(c) is much more complicated and it cannot be fully assigned by this superlattice. In addition, some diffraction spots are quite streaky. These phenomena reflect incommensurately the modulated nature of the structure, i.e., the atoms are deviated in complicated ways from their ideal positions which are expected from the simple shear operation. Also, as stated above, the substitutions of atoms seem to occur accompanied by the shear process. Further structure refinement including these details is hard to be done at the present stage. Considering the quite large superlattice and the complicated electron diffraction pattern, we need single-crystal diffraction data as a minimum requirement for the refinement. Although we are trying single-crystal growth for the present phase, we have not succeeded yet.

Magnetic measurements were carried out for the $Nd_{2.16}Ce_{0.225}CaCu_2O_{6.69}$ sample. Figs. 6 and 7 show the temperature dependence of the magnetic susceptibility and magnetization versus magnetic field (M–H) curves, respectively. The sample contained the impurity phases of Nd_2CuO_4, $NdCuO_{2.5}$ and CeO_2 although these phases are paramagnetic. In addition, we used the molecular weight for the formula of $Nd_{2.16}Ce_{0.225}CaCu_2O_{6.69}$ to calculate molar quantities, i.e., we supposed that the 0212-(Nd,Ce) phase has the same composition as the nominal mixture. This assumption and the presence of the impurity phases may cause experimental error of the magnetization data, but qualitative or quasi quantitative discussion below is not affected seriously by this uncertainty.

In the magnetic susceptibility data collected at 10 kOe, only one anomaly is seen near 150 K, and hysteresis between field cooling (FC) and zero-field cooling (ZFC)

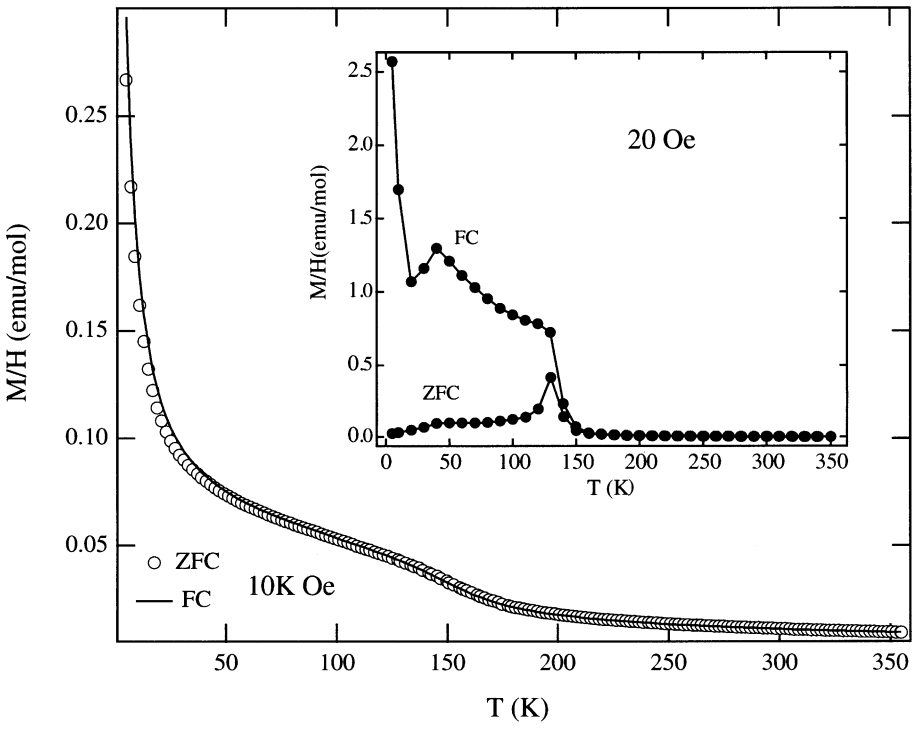

Fig. 6. Magnetic susceptibility data for the $Nd_{2.16}Ce_{0.225}CaCu_2O_{6.69}$ sample.

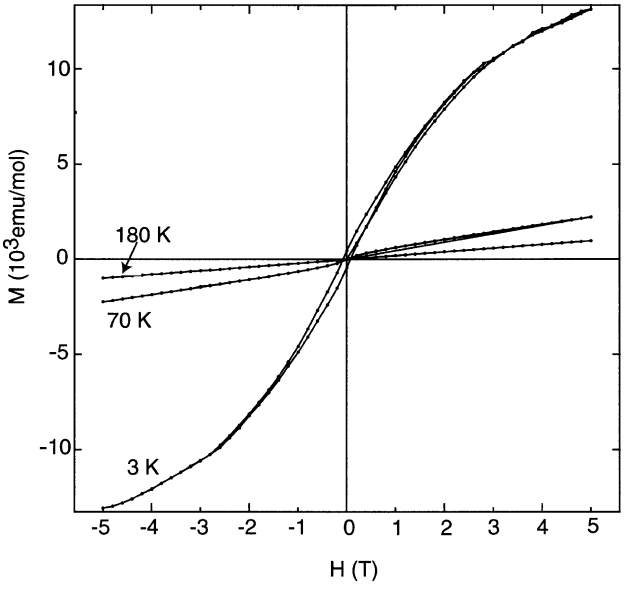

Fig. 7. Magnetization versus magnetic field (M–H) curves measured at 180, 70, and 3 K for the $Nd_{2.16}Ce_{0.225}CaCu_2O_{6.69}$ sample.

data is not detectable. At the applied magnetic field of 20 Oe, quite large difference is seen between the FC and ZFC data below ca. 130 K at which the ZFC curve takes the maximum. Three anomalies are seen in the FC magnetic susceptibility data; a steep increase at 150 K, down turn with a peak at 40 K and upturn with the minimum at 20 K. In the M–H curves in Fig. 7, magnetization increases linearly with the magnetic field at 180 K while non-linear behavior appears at 70 K, and magnetic hysteresis is clearly observed at 3 K with a residual magnetization of $\sim$460 emu/mol.

It has been reported that T'-R_2CuO_4 (R = heavy rare earth elements and Y) phases present a weak ferromagnetic component associated with the antiferromagnetic order of the Cu spins [12–20] and Dzyaloshinsky–Moriya interaction [21] between neighboring Cu moments is responsible for this behavior, i.e., canted spins in the CuO_2 planes form the origin of the weak ferromagnetism. The magnetic data for the present 0212-(Nd,Ce) phase suggest that it also undergoes a weak ferromagnetic transition near 150 K and the difference between FC and ZFC data is caused by frozen magnetic domains in the ZFC condition.

As stated above, the present phase has a complicated structure with incommensurate modulations. However, the basic nature of the structure can be understood as the result of shear operation for the $Nd_2CaCu_2O_6$ structure. In spite of the shear operation, the phase contains the CuO_2 plane, though it may not be the perfect plane, as well as T'-R_2CuO_4. The 150 K transition seems to be associated with the antiferromagnetic order of the Cu spins in the CuO_2 planes and their canting. The canting of spins is inconsistent with the tetragonal symmetry and usually weak ferromagnetism is a result of the reduction of the symmetry from tetragonal to orthorhombic, i.e., local crystal distortions are required in order to have a nonzero interaction. The

shear structure of the present phase can be the origin of the structural distortion.

At the present stage, the complicated magnetic behavior below ≈ 40 K is not elucidated, but it may be related to a second canting moment. According to this assumption, the downturn at 40 K and upturn at 20 K in the FC susceptibility curve can be explained as follows. At 150 K, the first canting moment is formed and it tends to be aligned parallel to the external magnetic fields with decreasing temperature. Near 40 K, the second canting moment is formed but its direction is inclined against that of the first canting moment with an angle larger than 90°. Finally, in the low-temperature region below ≈ 20 K, the second canting moment also tends to be aligned parallel to the external magnetic field. The second canting moment may be caused by the Nd and/or Cu spins which are placed outside the CuO_2 plane.

4. Conclusion

We performed phase search experiments for the Ce-containing system of Nd–Ce–Ca–Cu–O using the high-pressure synthesis technique. The Ce-doping brought about unexpected effects and a new phase of $(Nd,Ce)_{2+x}CaCu_2O_{6+y}$ was formed. X-ray diffraction studies and HRTEM observations indicated that it has a complicated shear structure based on the tetragonal $Nd_2CaCu_2O_6$-type structure. This phase showed a weak ferromagnetic transition at 150 K. This transition seems to be ascribed to the antiferromagnetic ordering and canting of Cu spins in the CuO_2 plane. Below ≈ 40 K, complicated magnetic behavior was observed suggesting the presence of a second weak ferromagnetic transition near 40 K due to the Nd and/or Cu spins placed outside the CuO_2 plane.

Acknowledgments

The authors thank M. Akaishi and S. Yamaoka of NIMS for their helpful suggestions on high-pressure synthesis. They also thank K. Kosuda and K. Natori for technical assistance. This work was supported by the Multi-Core Project, the COE Project, the Special Coordination Fund of the Science and Technology Agency and the Technical Specialist Supporting Program by JRDC.

References

[1] J.G. Bednorz, K.A. Müller, Z. Phys. B 64 (1986) 189.
[2] N. Nguyen, L. Er-Rakho, C. Michel, J. Choisnet, B. Raveau, Mater. Res. Bull. 15 (1980) 891.
[3] N. Nguyen, C. Michel, F. Studer, B. Raveau, Mater. Chem. 7 (1982) 413.
[4] N. Nguyen, J. Choisnet, B. Raveau, Mater. Res. Bull. 17 (1982) 567.
[5] R.J. Cava, B. Batlogg, R.B. van Dover, J.J. Krajewski, J.V. Waszczak, R.M. Fleming, W.F. Peck Jr., L.W. Pupp Jr., P. Marsh, A.C.W.P. James, L.F. Schneemeyer, Nature. 345 (1990) 602.
[6] K. Kinoshita, H. Shibata, T. Yamada, Physica C 171 (1990) 523.
[7] M. Isobe, Y. Matsui, E. Takayama-Muromachi, in: S. Nakajima, M. Murakami (Eds.), Advances in Superconductivity *IX*, Springer Verlag, Tokyo, 1997, p. 353.
[8] Hk. Müller-Buschbaum, W. Wollschlager, Z. Anorg. Allg. Chem. 414 (1975) 76.
[9] B.H. Chen, D. Walker, E. Suard, B.A. Scott, B. Mercey, M. Hervieu, B. Raveau, Inorg. Chem. 34 (1995) 2077.
[10] Z. Hiroi, M. Takano, Nature 377 (1995) 41.
[11] Z. Hiroi, J. Solid State Chem. 123 (1996) 223.
[12] J.D. Thompson, S-W. Cheong, S.E. Brown, Z. Fisk, S.B. Oseroff, M. Tovar, D.C. Vier, S. Schultz, Phys. Rev. B 39 (1989) 6660.
[13] H. Okada, M. Takano, Y. Takeda, Phys. Rev. B 42 (1990) 6813.
[14] S.B. Oseroff, D. Rao, F. Wright, D.C. Vier, S. Schultz, J.D. Thompson, Z. Fisk, S-W. Cheong, M.F. Hundley, M. Tovar, Phys. Rev. B 41 (1990) 1934.
[15] M. Tovar, X. Obradors, F. Pérez, S.B. Oseroff, R.J. Duro, J. Rivas, D. Chateigner, P. Bordet, J. Chenavas, J. Appl. Phys. 70 (1991) 6095.
[16] R.D. Zysler, M. Tovar, C. Rettori, D. Rao, H. Shore, S.B. Oseroff, D.C. Vier, S. Schultz, Z. Fisk, S-W. Cheong, Phys. Rev. B 44 (1991) 9467.
[17] M. Tovar, X. Obradors, F. Pèrez, S.B. Oseroff, R.J. Duro, J. Rivas, D. Chateigner, P. Bordet, J. Chenavas, Phys. Rev. B 45 (1992) 4729.
[18] H.D. Yang, T.H. Meen, Y.C. Chen, Phys. Rev. B 48 (1993) 7720.
[19] M.K. Crawford, R.L. Harlow, E.M. McCarron, W.E. Farneth, N. Herron, H. Chou, D.E. Cox, Phys. Rev. B 47 (1993) 11623.
[20] J.F. Vente, P.D. Battle, Phys. Rev. B 58 (1998) 2699.
[21] I. Dzyaloshinski, J. Phys. Chem. Solids 4 (1958) 241; T. Moriya, Phys. Rev. 120 (1960) 91.